ACS APPLIED MATERIALS & INTERFACES

Research Article

www.acsami.org

Enhancement Effects of Cobalt Phosphate Modification on Activity for Photoelectrochemical Water Oxidation of TiO_2 and Mechanism Insights

Dening Liu,[†] Liqiang Jing,*[,†] Peng Luan,[†] Junwang Tang,[‡] and Honggang Fu*[,†]

[†]Key Lab of Functional Inorganic Materials Chemistry, Ministry of Education, School of Chemistry and Materials Science, Heilongjiang University, Harbin 150080, China

[‡]Department of Chemical Engineering, University College London, Torrington Place, London WC1E 7JE, United Kingdom

Supporting Information

ABSTRACT: Cobalt phosphate-modified nanocrystalline TiO_2 (nc-TiO_2) films were prepared by a doctor blade method using homemade nc-TiO_2 paste, followed by the post-treatments first with monometallic sodium orthophosphate solution and then with cobalt nitrate solution. The modification with an appropriate amount of cobalt phosphate could greatly enhance the activity for photoelectrochemical (PEC) water oxidation of nc-TiO_2, superior to the modification only with the phosphate anions. It is clearly demonstrated that the enhanced activity after cobalt phosphate modification is attributed to the roles of cobalt(II) ions linked by phosphate groups with the surfaces of nc-TiO_2 mainly by means of the surface photovoltage responses in N_2 atmosphere. It is suggested that the linked cobalt(II) ions could capture photogenerated holes effectively to produce high-valence cobalt ions, further inducing oxidation reactions with water molecules to rereturn to cobalt(II) ions. This work is useful to explore feasible routes to improve the performance of oxide-based semiconductors for PEC water splitting to produce clean H_2 energy.

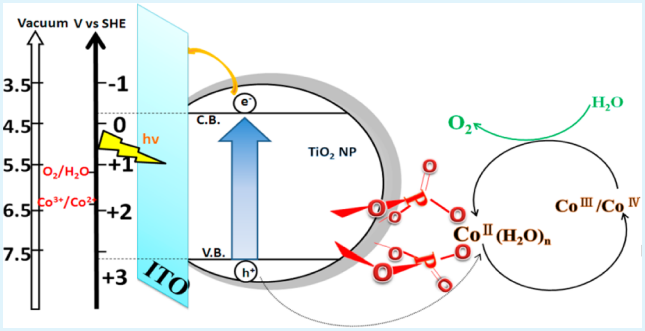

KEYWORDS: *TiO_2, cobalt phosphate modification, photogenerated charge separation, atmosphere-controlled surface photovoltage spectroscopy, photoelectrochemical water oxidation*

INTRODUCTION

To realize the sunlight renewable and carbon neutral energy source of sufficient scale to replace fossil fuels, meeting rising global energy demand,[1] it is desirable to find a method to efficiently convert and store solar energy. Actually, nature provides the blueprint for storing sunlight in the form of chemical fuels.[1,2] The basic steps of natural photosynthesis involve the absorption of sunlight and then its conversion into spatially separated electron−hole pairs.[3,4] The emergence of successful photoelectrochemical (PEC) technologies is to use solar photons to drive the chemistry of splitting H_2O molecules to generate O_2 and H_2, leading to the storage of the photon energy in the chemical bond of H_2.[5,6] This overall transformation can be involved with two separate half reactions: the two-electron reduction of water to H_2 and the four-electron oxidation of water to O_2.[7,8]

Although TiO_2 could only absorb the UV light, it has been extensively studied as the most useful material for photocatalytic purpose because of its high photocatalytic activity, chemical stability, nontoxicity, and low cost.[9−12] The efficiency of photocatalytic reactions, including water splitting for H_2 production, largely depends on three factors: effective optical absorption by the photocatalyst, effective creation of charger carriers, and effective use of the charge carriers in the photocatalytic processes. UV light and visible light constitute approximately 47% of solar irradiation,[13] which makes the target photocatalytic efficiency of more than 10% challenging.

One extensively cited study[14] has reported that 90% of photoelectrons and photoholes recombine within 10 ns, and several other studies also show 60−80% of electrons recombine with holes on a nanosecond time scale in TiO_2 colloid.[15,16] Tamaki et al observed that the geminate recombination of electron and hole did not take place before 1 ns under weak laser intensity in air.[17] Yamakata et al reported that O_2 production occurred on the second time scale, much slower than H_2 production, which happens on the hundreds of microsecond time scale.[18] Tang et al. suggested that the oxygen production take ∼1 s.[8] These indicate that the reactions between photogenerated holes and water molecules mainly limit the performance of PEC water splitting.[19−22]

Recently, our group has demonstrated that the phosphate modification changes the surface-carried charge properties of

Received: September 13, 2012
Accepted: April 25, 2013
Published: April 25, 2013

nc-TiO_2 in neutral water so as to promote the separation of photogenerated carriers, leading to the enhanced activity for PEC water oxidation. However, the phosphate groups modified on the surfaces of TiO_2 do not catalyze the reactions between photogenerated holes and water molecules.[19] Notably, Matthew et al reported an oxygen-evolving catalyst formed in situ upon anodic polarization of an inert electrode in neutral aqueous phosphate solutions containing Co^{2+},[23] and a photoassisted approach was used to deposit cobalt phosphate onto the mesostructured α-Fe_2O_3 as good-performance photoanodes.[24] It is generally assumed that the cobalt ions should play important roles as catalysts of water oxidation,[25,26] and few papers are involved with the phosphate role. Thus, the mechanism for the activity enhancement in PEC water oxidation is poorly understood. Unexpectedly, the studies on the cobalt phosphate modified nc-TiO_2 as efficient PEC electrodes for water oxidation have seldom been investigated to date.

On the basis of the previous study on the phosphate-modified TiO_2,[19] along with the phosphate groups as effective linkers,[19,27] it is meaningful to further carry out the investigation on the cobalt phosphate-modified TiO_2, aiming to greatly improve the activity for PEC water oxidation and simultaneously to reveal the activity-enhanced mechanism in detail. In particular, the atmosphere-controlled surface photovoltage technique developed recently in our group as an powerful tool is to be used to explore the photogenerated charge properties of modified TiO_2,[28−30] which is much favorable to disclose the roles of cobalt and phosphate groups in the PEC water oxidation.

In this work, the effects of cobalt phosphate modification on the properties of photoinduced charges of the resulting nc-TiO_2 films were investigated in details mainly by means of atmosphere-controlled surface photovoltage techniques, and electrochemical measurements in the light or in the dark. It is demonstrated that the modification with cobalt phosphate could improve the photoinduced charge separation of nc-TiO_2 by cobalt(II) cations effectively capturing holes to produce high-valence cobalt cations with strong oxidation ability, and the phosphate anions play important roles as effective linkers between nc-TiO_2 and cobalt cations. This is well responsible for the enhanced activity for PEC water oxidation of modified nc-TiO_2 film under ultraviolet irradiation and its activity stability. This work would provide feasible routes to design and synthesize high-performance TiO_2-based PEC nanomaterials for water splitting.

EXPERIMENTAL SECTION

Synthesis of Materials. At first, the nanocrystalline titanium dioxide (nc-TiO_2) paste was prepared as follows. One g of synthesized TiO_2 nanopowder was dispersed in 2 mL of iso-propyl alcohol, and then treated by an ultrasonic process for 30 min and stirring for 30 min. After that, 0.5 g of the analytical grade of Macrogol-6000, which is 1,2-ethanediol homopolymer with the molecular weight of about 6000, was added to the above system, and then retreated by an ultrasonic process for 30 min and stirring for 30 min. Finally, 0.1 mL of acetylacetone was introduced to the above mixture, followed by an ultrasonic treatment and continuously stirring for at least 1 day. Conductive indium tin oxide (ITO)-coated glasses, used as the substrates for the nc-TiO_2 films, were cleaned by sonicating in acetone for 30 min and then in deionized water for another 30 min prior to use. Nc-TiO_2 film was prepared by the doctor blade method using Scotch tape as the spacer. Following drying in air for 10 min, films were sintered at 723 K for 30 min. The resulting film was an average 4 μm thick checked by a profilometer. Subsequently, the resulting film was put into a 0.1 M monometallic sodium orthophosphate solution for 1 h. After that, the film was rinsed with deionized water and dried naturally in air for 0.5 h, then sintered at 723 K for 30 min. When its temperature goes down to the room temperature, the resulting film was put into a desired-concentration monometallic cobalt nitrate solution for 1 h. After the film was rinsed with deionized water and dried naturally in air for 0.5 h, a vacuum drying treatment at 313 K is employed for 6 h. The ITO covered by TiO_2 film was cut into approximately 1.0 cm × 3.0 cm pieces with TiO_2 film surface area of 1.0 cm × 1.0 cm. To make a photoelectrode, an electrical contact was made with ITO substrate by using silver conducting paste connected to a copper wire, which was then enclosed in a glass tube. The working geometric surface area of TiO_2 was 1.0 cm × 1.0 cm where the remaining area was covered by epoxy resin.

Characterization of Films. The film samples were characterized by X-ray powder diffraction (XRD) with a Rigaku D/MAX-rA powder diffractometer (Japan), using Cu$K\alpha$ radiation (α = 0.15418 nm), and an accelerating voltage of 30 kV and emission current of 20 mA were employed. Scanning electron microscopy (SEM) observations were carried out on a Philips XL-30-ESEM-FEG operated at an accelerating voltage of 20 kV. Atomic force microscopy (AFM) images were recorded on a Seiko SPA 400 with a Nanonavi Probe Station in tapping mode (dynamic force mode). Commercially available Si cantilevers with a force constant of 20 N/m were used as substrate. The ultraviolet−visible absorption spectra of the samples were recorded with a model Shimadzu UV2550 spectrophotometer. The Fourier transform infrared spectra (FT-IR) of the samples were collected with a Bruker Equinox 55 Spectrometer, using KBr as diluents. The surface composition and elemental chemical state of the samples were examined by X-ray photoelectron spectroscopy (XPS) using a Kratos−AXIS ULTRA DLD apparatus with Al(Mono) X-ray source, and the binding energies were calibrated with respect to the signal for adventitious carbon (binding energy = 284.6 eV). The surface photovoltage spectroscopy (SPS) measurement of the sample was carried out with a home-built apparatus that has been described elsewhere.[31,32] Monochromatic light was obtained by passing light from a 500 W xenon lamp (CHFXQ500W, Global Xenon Lamp Power, made in China) through a double-prism monochromator (Hilger and Watts, D 300, made in England). A lock-in amplifier (SR830, made in the U.S.A.), synchronized with a light chopper (SR540, made in U.S.A.), was employed to amplify photovoltage signal. The powder sample was sandwiched between two ITO glass electrodes by which the outer electric field could be employed, and the sandwiched electrodes were arranged in an atmosphere-controlled container with a quartz window.

Photoelectrochemical Experiments. PEC experiments were performed in a glass cell using a 500 W xenon light, with a stabilized current power supply as the illumination source and 0.5 M $NaClO_4$ solution as neutral electrolyte. The working electrode was the nc-TiO_2 film (illumination area about 1.0 cm^2), illuminated from the ITO glass side. Platinum wire (99.9%) was used as the counter electrode, and a saturated KCl Ag/AgCl electrode (SSE) was used as the reference electrode. All the potentials in the paper will be referred to SSE at 298K. Oxygen-free nitrogen gas was used to bubble through the electrolyte before and during the experiments. Applied potentials were controlled by a commercial computer-controlled potentiostat (LK2006A made in China). For comparison, the current was also measured on dark condition.

RESULTS AND DISCUSSION

Structural Characterization. The XRD peaks at 2θ = 25.28° (A101) and 2θ = 27.40° (R110) are often taken as the characteristic peaks of anatase and rutile crystal phase of TiO_2, respectively.[33] The crystallite size can be determined from the broadening of corresponding X-ray diffraction peak by Scherrer formula.[34] It is confirmed from Figure 1 that the TiO_2 film (TF) has an entire anatase phase with an average crystallite size of about 10 nm. Compared with the XRD patterns of TF, those

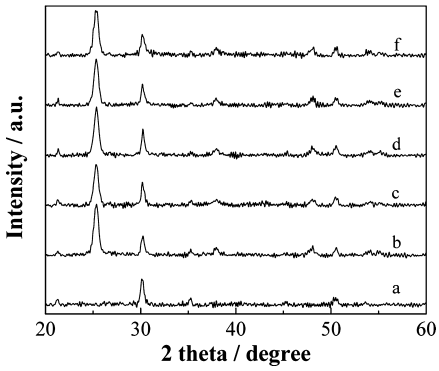

Figure 1. XRD patterns of different modified nc-TiO_2 films: (a) ITO glass, (b) TiO_2, (c) PTF, (d) 2×10^{-3} Co-PTF, (e) 5×10^{-3} Co-PTF, (f) 8×10^{-3} Co-PTF.

of phosphate modified TF (PTF) and of cobalt phosphate modified TF (Co-PTF) do not nearly change, indicating the phosphate and cobalt phosphate modification does not influence the phase composition and crystallinity of TiO_2. Similarly, it is also demonstrated from Raman spectra (see Figure S1 in the Supporting Information), AFM images in Figure 2, SEM images in Figure 3 and UV−vis absorption spectra in Figure 4 that the cobalt phosphate modification does not influence crystalline phase, surface microstructure and optical absorption behavior of the TF. In the FT-IR spectra (see Figure S2 in the Supporting Information), the IR band centering at 800 cm^{-1} corresponds to the Ti−O−Ti stretching vibration mode in crystal TiO_2,[30] and the IR peaks at about 1630 and 3400 cm^{-1} are ascribed to surface hydroxyl and adsorbed water molecules, respectively.[34] Compared with the TF, a new broad IR band appears at 1010−1250 cm^{-1} in the phosphate-modified TF, attributable to the phosphate in a bidentate state of ligation.[27,35]

Figure 5 shows XPS spectra of Ti 2p (A), O 1s (B), P 2p (C), and Co 2p (D) of the TF, PTF, and Co-PTF samples, and their atomic percentage contents of Ti, P, and Co on the surfaces are listed in the table S1 in the Supporting Information. The strong Ti $2p_{3/2}$ XPS peak at about 458.4 eV is attributed to Ti^{4+}.[36] The O 1s XPS spectra are wide and asymmetric, demonstrating that there are at least two kinds of O chemical states according to the binding energy range from 528.0 to 533.0 eV,[37] including crystal lattice oxygen (O_L) and hydroxyl oxygen (O_H) with increasing binding energy. One can see that the binding energy of P 2p is 133.2 eV, which is characteristic of P in the phosphate group.[38] Thus, it is confirmed that P exists as the form of $[PO_4]^{3-}$, which is in good agreement with IR results. As expected, the binding energy peak of Co $2p_{3/2}$ at 781.2 eV, along with a satellite peak at 786.2 eV, implies that Co is mainly +2 valence.[39,40] Therefore, it is confirmed that the cobalt(II) phosphate is successfully modified on the surfaces of TF.

Photoinduced Charge Properties. The SPS method, with a very high sensitivity, is a well-established contactless and nondestructive technique for semiconductor characterization that relies on analyzing illumination-induced changes in the surface voltage.[30−32,41−44] It can reflect photogenerated charge separation and transfer behavior as well as optical absorption characteristics of semiconductor samples, especially for the atmosphere-controlled SPS responses.[44] Figure 6 shows the SPS responses of unmodified and modified TiO_2 nanoparticles in different atmospheres. For the three samples, an obvious SPS response, with a SPS peak at about 345 nm, can be found at the wavelength range from 300 to 370 nm, which is mainly attributed to the electronic transitions from the valence band to the conduction band (O 2p→Ti 3d).[30,32,43] During the process of SPS measurement, the ITO glass can strongly absorb the light with the wavelength lower than 340 nm, which results in a corresponding weak or even no SPS signal.[31]

Noticeably, the SPS response of unmodified TiO_2 becomes gradually weak as decreasing the content of O_2 in atmosphere. According to the SPS principle that the surface photovoltage signal of solid semiconductor material mainly results from the photogenerated charges, followed by the separation under the built-in electric field and/or via the diffusion process,[43,44] the SPS response of nanosized TiO_2 should mainly originate from the photogenerated charge separation via the diffusion process since the built-in electric fields of nanomaterials are usually neglected. Thus, it is expected that the positive photogenerated holes can preferentially diffuse to the surfaces of testing electrode by the adsorbed O_2 capturing effectively photogenerated electrons.[44] Therefore, the presence of O_2 is necessary for the SPS occurrence. By comparison, it is confirmed that the phosphate modification does not change the SPS attribute of TiO_2. Differently from TiO_2, the cobalt phosphate-modified TiO_2 exhibits much stronger SPS response in N_2 than in O_2-containing atmosphere, indicating that the photogenerated holes are obviously captured. Naturally, it is deduced that the cobalt phosphate linked on the surfaces of TiO_2 could capture photogenerated holes effectively, which is favorable to improve the charge separation.

Photoelectrochemical Performance. Because the photoinduced holes could be trapped by the modified cobalt phosphate, it is hypothesized that the photocurrent density of TF would be enhanced by modifying with cobalt phosphate. Figure 7 shows the current−voltage curves of TF, PTF and Co-PTF in neutral electrolyte in the dark and under UV

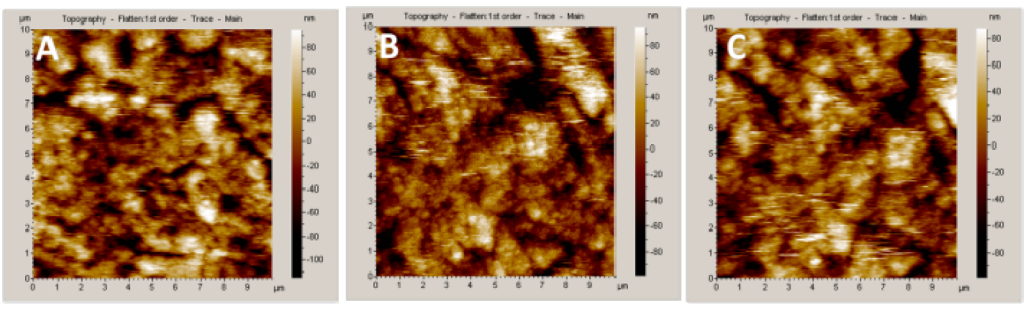

Figure 2. AFM images of different treated nc-TiO_2 film. (A is unmodified, B is phosphate-modified, C is cobalt phosphate-modified).

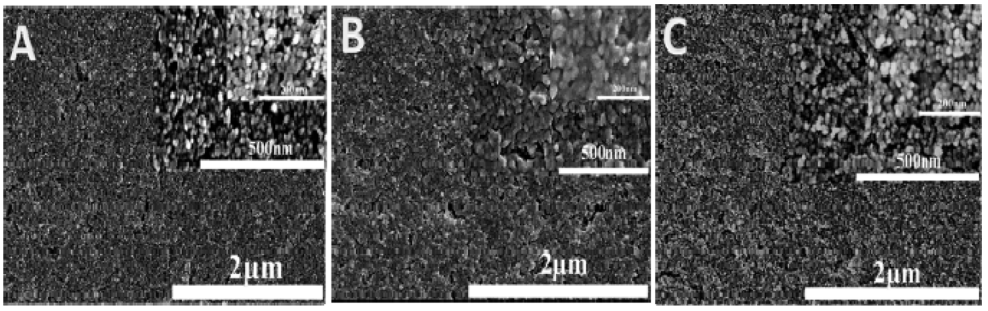

Figure 3. SEM images of different treated nc-TiO_2 film. (A is unmodified, B is phosphate-modified, C is cobalt phosphate-modified, inset shows the corresponding image with high magnification).

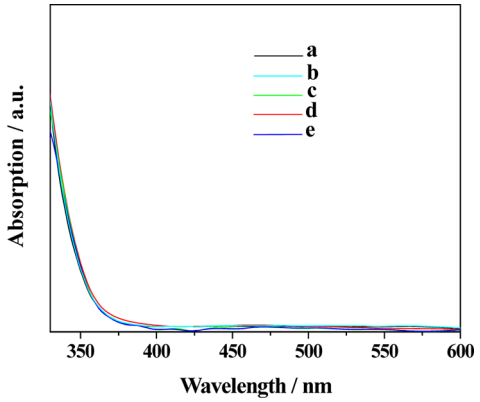

Figure 4. UV−vis spectra: (a) TF, (b) PTF, (c) 2×10^{-3} Co-PTF, (d) 5×10^{-3} Co-PTF, (e) 8×10^{-3} Co-PTF).

illumination. Different from in the dark, the onset voltage of TF under UV illumination is about at −0.4 V, and the photocurrent quickly increases as the used voltage rises.[45] This is because that the increase in the bias is much favorable to enhance the separation situation of photogenerated charges of TF. However, the photocurrent increases slowly when the bias is over −0.3 V. In this case, the separation situation of photoinduced charges of TF would not greatly be enhanced or nearly keep stable, resulting in a small enhancement in the photocurrent.[24]

Compared to the TF, the phosphate-modified TF exhibits a strong photocurrent, which is attributed to the formed negative electric field in the surface layer of TiO_2 promoting photogenerated charge separation.[19] And also, the TF modified with an appropriate amount of cobalt phosphate displays a much strong photocurrent, even stronger than the TF modified with phosphate. Interestingly, the TF modified with cobalt phosphate performs at a low overpotential for water oxidation

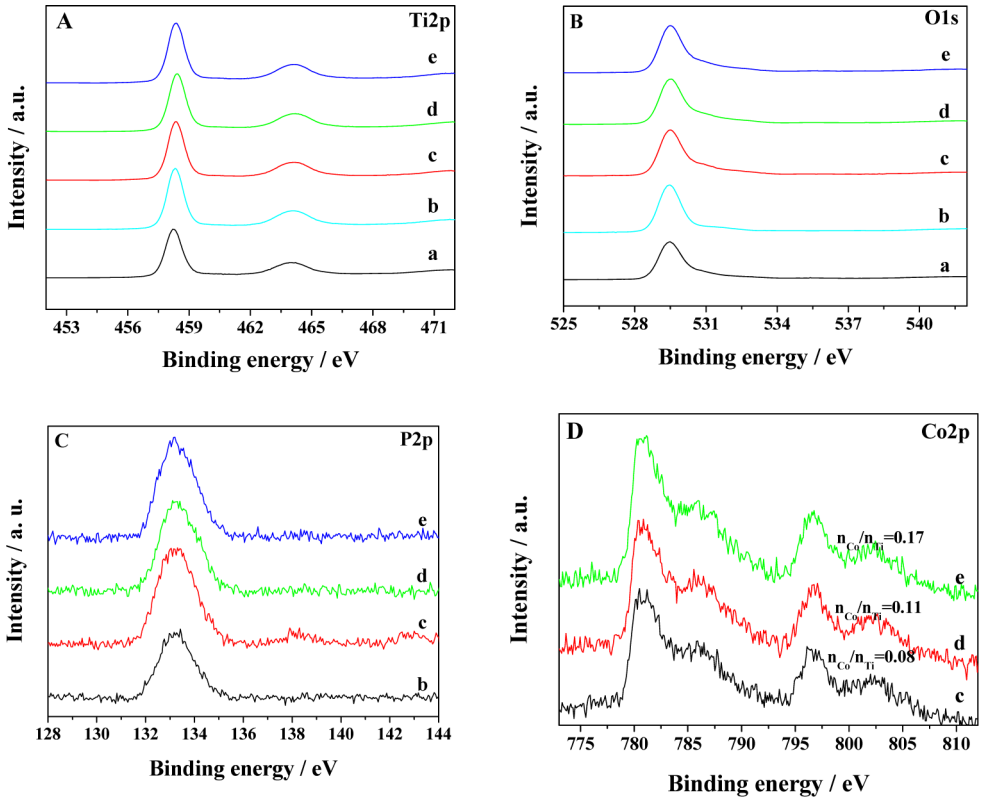

Figure 5. XPS spectra of (A) Ti 2p, (B) O 1s, (C) P 2p, (D) Co 2p ((a) TF, (b) PTF, (c) 2×10^{-3} Co-PTF, (d) 5×10^{-3} Co-PTF, (e) 8×10^{-3} Co-PTF).

dx.doi.org/10.1021/am400351m | ACS Appl. Mater. Interfaces 2013, 5, 4046−4052

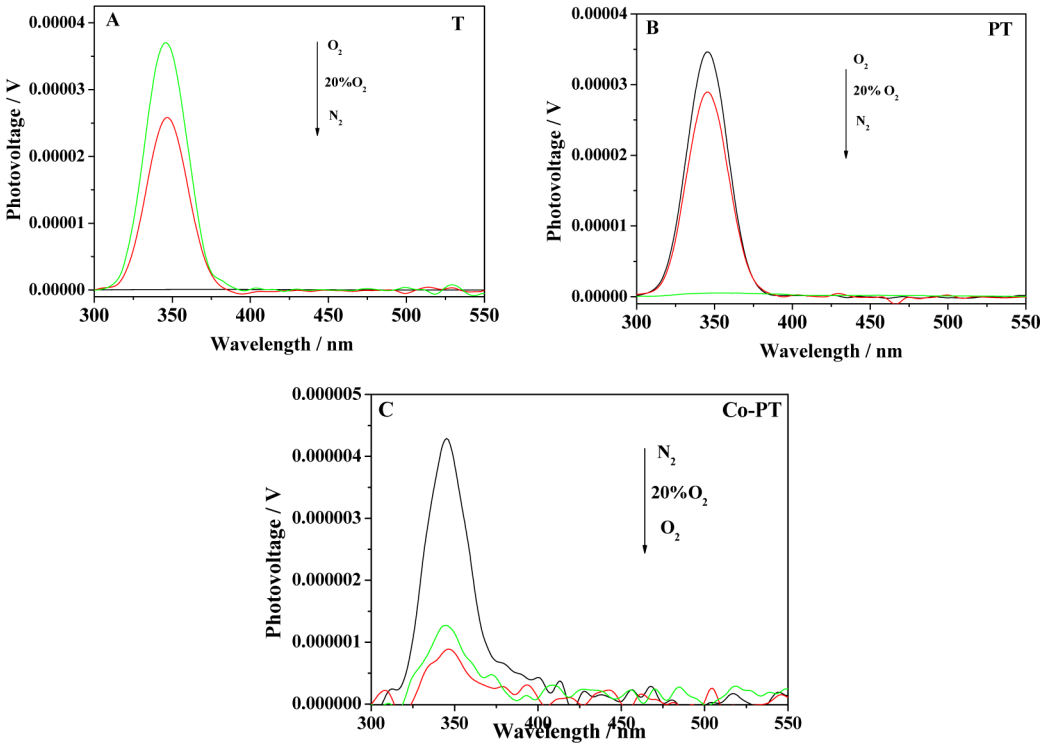

Figure 6. SPS responses of (A) unmodified, (B) phosphate-modified, and (C) cobalt phosphate-modified nc-TiO_2 in different atmospheres.

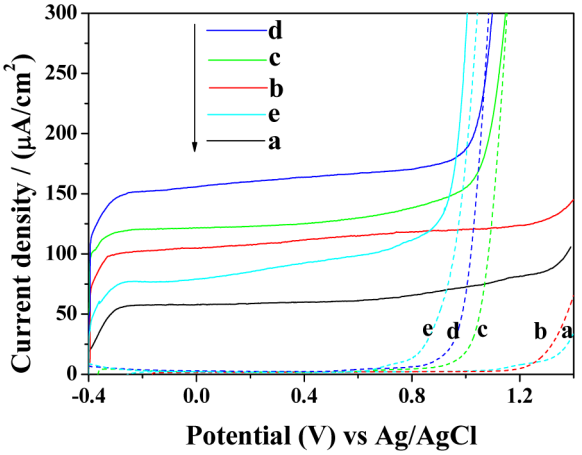

Figure 7. *I*−*V* curves under illumination (solid line) and in the dark (dash line). Potentials are measured against a Ag/AgCl (saturated KCl) reference electrode in a nitrogen purged 0.5 M $NaClO_4$ (aq) solution. (a) TF, (b) PTF, (c) 2×10^{-3} Co-PTF, (d) 5×10^{-3} Co-PTF, (e) 8×10^{-3} Co-PTF).

to produce O_2 in the dark. This is possibly related to the roles of cobalt ions as electrochemical catalyst.[23,46] In addition, it is demonstrated that the cobalt phosphate modified TFs are stable according to the current−time curves (see Figure S3 in the Supporting Information).

To further prove the above result, incident-photon-to-current-efficiencies (IPCE) for TF, PTF, and Co-PTF were measured at 0 V vs SSE as a function of incident light wavelength (see figure S4 in the Supporting Information). IPCE is expressed as IPCE = $(1240I)/(\lambda J_{light})$, where I is the photocurrent density ($\mu A/cm^2$), λ is the incident light wavelength (nm), and J_{light} ($\mu W/cm^2$) is the power density of monochromatic light at a specific wavelength. One could note that the Co-PTF shows substantially enhanced IPCE value compared to the TF and PTF at all measured wavelengths, which is consistent with their *I*−*V* characteristics. Their IPCE values drop to zero at wavelengths about above 390 nm, in accordance with the band gap of TiO_2.[47]

Discussion. On the basis of the above results, it is suggested that the obvious increase in the photocurrent of TF after modification with a proper amount of cobalt phosphate is attributed to the two factors. One factor is to improve photogenerated charge separation by cobalt phosphate modification, based on the above SPS results. Thus, it is expected that the cobalt(II) ions linked on the surfaces of TF could capture photogenerated holes to further form high-valence cobalt ions. The other is to further induce water oxidation reactions to produce O_2 by the produced high-valence cobalt ions, mainly based on the thermodynamic data (Co^{3+}/Co^{2+} = 1.746 V vs NHE, pH 7).[48] After that, the cobalt ion is returned back to the low valence (II).

To further support the points, we have carried out the comparative study on the cobalt phosphate modified TF treated at 313K and 723K. Differently, the cobalt exists mainly as the form of Co_3O_4 after treatment at 723K based on the Raman spectra (see Figure S5 in the Supporting Information).[49] This is well responsible for the obvious optical absorption at 400−600 nm according to the UV−vis spectra (see Figure S6 in the Supporting Information). As a result, the photocurrent of cobalt phosphate modified TF is obviously decreased after thermal treatment at 723K (see Figure S7 in the Supporting Information), even lower than that of TF. Based on the low current response in dark, it is deduced that the formed Co_3O_4 is unfavorable to catalyze the water oxidation and transport charge. This leads to the greatly decreased photocurrent of modified TF after high-temperature treatment.

In addition, we also compare the cobalt phosphate modified and cobalt ion modified TF, as shown in figure S8 in the

dx.doi.org/10.1021/am400351m | ACS Appl. Mater. Interfaces 2013, 5, 4046−4052

Supporting Information. One can see that the two modified TFs exhibit stronger photocurrent than the unmodified TF at 0 V vs SSE. And also, the cobalt phosphate modified TF is stable, while the cobalt ions modified one is not stable. This clearly demonstrates that the phosphate groups would effectively connect the cobalt ions with the surfaces of TF. In particular, the phosphate groups could transport photogenerated charge.[19] Thus, the mechanism scheme on the enhanced photocurrent of TF after modification with cobalt phosphate is drawn, as shown in Figure 8. The key of the suggested mechanism is the roles of

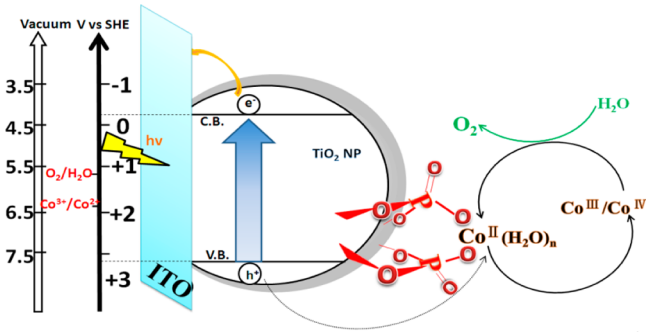

Figure 8. Mechanism schematic of cobalt phosphate modified nc-TiO_2 for water oxidation.

cobalt(II) ions effectively linked on the surfaces of TiO_2 via phosphate groups, involved with its capturing photogenerated holes and then inducing water oxidation reactions. The photocurrent enhancement implies that the activity for PEC water oxidation is improved. Therefore, it is suggested that the cobalt phosphate modification would be applicable to other oxide semiconductors investigated widely as efficient photocatalysts, such as ZnO, Fe_2O_3, and $BiVO_4$.[50−56]

CONCLUSIONS

On the basis of our previous work that the phosphate modification could improve the activity for PEC water oxidation of TF, along with the result that the reactions between photogenerated holes and water molecules are rather slow, we have further carried out this study on the cobalt phosphate modified TF. It is demonstrated that the activity for the PEC water oxidation of TF is greatly improved by modification with a proper amount of cobalt phosphate, even higher than that of TF modified with phosphate. It is suggested that the key of the activity-enhanced mechanism lies in the role of cobalt(II) ion linked by phosphate groups with the TiO_2 surface. The phosphate groups could make cobalt ions connected to the surfaces of TiO_2, and transport charge. And, the linked cobalt(II) ions could effectively capture photogenerated holes to form high-valence Co ions so as to promote charge separation, and the produced high-valence Co ions would easily induce the water oxidation reactions to evolve O_2, simultaneously rechanging into the state of +2 valence. This work would provide us with new ideas to improve the performance of PEC water splitting of oxide-based semiconductors to produce clean H_2 energy, for example by substitution of Co ions with other metallic ions, or substitution of −O−P−O− groups with −O−Si−O− groups as linkers.

ASSOCIATED CONTENT

Supporting Information

Raman spectra (Figures S1 and S5), atomic content (Table S1), Fourier transform infrared spectra (Figure S2), *I*−*T* curves (Figures S3 and S8), IPCE spectra (Figure S4), UV−vis spectra (Figure S6), *I*−*V* curves (Figure S7). This material is available free of charge via the Internet at http://pubs.acs.org/.

AUTHOR INFORMATION

Corresponding Author

*E-mail: Jinglq@hlju.edu.cn (L.J.).

Notes

The authors declare no competing financial interest.

ACKNOWLEDGMENTS

We are grateful for financial support from NSFC (21071048), the Program for Innovative Research Team in Chinese Universities (IRT1237), the Specialized Research Fund for the Doctoral Program of Higher Education (20122301110002), and the Chang Jiang Scholar Candidates Programme for Heilongjiang Universities (2012CJHB003), and the Science Foundation of Harbin City of China (2011RFXXG001). Special thanks is given to Prof. Jame R Durrant at Imperial College London for his valuable discussion on the activity-enhanced mechanism.

REFERENCES

(1) Lewis, N. S.; Nocera, D. G. *Proc. Natl. Acad. Sci. U.S.A.* **2006**, *103*, 15729−15735.
(2) Nelson, N.; Ben-Shem, A. *Nat. Rev. Mol. Cell Biol.* **2004**, *5*, 971−982.
(3) Barber, J. *Philos. Trans. R. Soc. London, Ser. A* **2007**, *365*, 1007−1023.
(4) Bard, A. J.; Fox, M. A. *Acc. Chem. Res.* **1995**, *28*, 141−145.
(5) Grätzel, M. *Nature* **2001**, *414*, 338−344.
(6) Grimes, C. A.; Varghese, O. K.; Ranjan, S. *Light, Water, Hydrogen: The Solar Generation of Hydrogen by Water Photoelectrolysis*; Springer, New York, 2007.
(7) Turner, J. A. *Science* **2004**, *305*, 972−974.
(8) Tang, J. W.; Durrant, J. R.; Klug, D. R. *J. Am. Chem. Soc.* **2008**, *130*, 13885−13891.
(9) Fujishima, A.; Honda, K. *Nature* **1972**, *238*, 37−38.
(10) Wang, R.; Hashimoto, K.; Fujishima, A.; Chikumi, M.; Kojima, E.; Kitamura, A.; Shimohigoshi, M.; Watanabe, T. *Nature* **1997**, *388*, 431−432.
(11) Linsebigler, A. L.; Lu, G.; Yates, J. T. *Chem. Rev.* **1995**, *95*, 735−758.
(12) Stathatos, E.; Petrova, T.; Lianos, P. *Langmuir* **2001**, *17*, 5025−5030.
(13) Zou, Z. G.; Ye, J. H.; Sayama, K.; Arakawa, H. *Nature* **2001**, *414*, 625−627.
(14) Serpone, N.; Lawless, D.; Khairutdinov, R.; Pelizzetti, , E. *J. Phys. Chem.* **1995**, *99*, 16655−16661.
(15) Leytner, S.; Hupp, J. T. *Chem. Phys. Lett.* **2000**, *330*, 231−236.
(16) Bahnemann, D. W.; Hilgendorff, M.; Memming, R. *J. Phys. Chem. B* **1997**, *101*, 4265−4275.
(17) Tamaki, Y.; Furube, A.; Murai, M.; Hara, K.; Katoh, R.; Tachiya, M. *Phys. Chem. Chem. Phys.* **2007**, *9*, 1453−1460.
(18) Yamakata, A.; Ishibashi, T.; Onishi, H. *J. Phys. Chem. B* **2001**, *105*, 7258−7262.
(19) Jing, L. Q.; Zhou, J.; Durrant, J. R.; Tang, J. W.; Liu, D. N.; Fu, H. G. *Energy Environ. Sci.* **2012**, *5*, 6552−6558.
(20) Aroutiounian, V. M.; Arakelyan, V. M. G. E. *Sol. Energy* **2005**, *78*, 581−592.
(21) Osterloh, F. E. *Chem. Mater.* **2008**, *20*, 35−54.

(22) Xiao-e, L.; Green, A. N. M.; Haque, S. A.; Mills, A.; Durtant, J. R. *J. Photochem. Photobiol. A* **2004**, *162*, 253−259.
(23) Kanan, M. W.; Nocera, D. G. *Science* **2008**, *321*, 1072−1075.
(24) Zhong, D. K.; Cornuz, M.; Sivula, K.; Grätzel, M.; Gamelin, D. R. *Energy Environ. Sci.* **2011**, *4*, 1759−1764.
(25) Zhong, D. K.; Gamelin, D. R. *J. Am. Chem. Soc.* **2010**, *132*, 4202−4207.
(26) Young, E. R.; Costi, R.; Paydavosi, S.; Nocera, D. G.; Bulović, V. *Energy Environ. Sci.* **2011**, *4*, 2058−2061.
(27) Zhao, D.; Chen, C. C.; Wang, Y. F.; Ji, H. W.; Ma, W. H.; Zang, L.; Zhao, J. C. *J. Phys. Chem. C* **2008**, *112*, 5993−6001.
(28) Cao, Y.; Jing, L. Q.; Shi, X.; Luan, Y. B.; Durrant, J. R.; Tang, J. W.; Fu, H. G. *Phys. Chem. Chem. Phys.* **2012**, *14*, 8530−8536.
(29) Jing, L. Q.; Xin, B. F.; Yuan, F. L.; Xue, L. P.; Wang, B. Q.; Fu, H. G. *J. Phys. Chem. B* **2006**, *110*, 17860−17865.
(30) Jing, L. Q.; Fu, H. G.; Wang, B. Q.; Wang, D. J.; Xin, B. F.; Li, S. D.; Sun, J. Z. *Appl. Catal., B* **2006**, *62*, 282−290.
(31) Lin, Y. H.; Wang, D. J.; Zhao, Q. D.; Yang, M.; Zhang, Q. L. *J. Phys. Chem. B* **2004**, *108*, 3202−3206.
(32) Jing, L. Q.; Sun, X. J.; Shang, J.; Cai, W. M.; Xu, Z. L.; Du, Y. G.; Fu, H. G. *Sol. Energy. Mater. Sol. Cells.* **2003**, *79*, 133−151.
(33) Sreethawong, T.; Suzuki, Y.; Yoshikawa, S. *J. Solid State Chem.* **2005**, *178*, 329−338.
(34) Ciesla, U.; Schacht, S.; Stucky, G. D.; Unger, K. K; Schueth, F. *Angew. Chem., Int. Ed.* **1996**, *35*, 541−547.
(35) László, K.; Szilvia, P.; Imre, B.; Imre, D. *Chem. Mater.* **2007**, *19*, 4811−4819.
(36) Alfaya, A. A. S.; Gushikem, Y.; Castro, S. C. de. *Chem. Mater.* **1998**, *10*, 909−913.
(37) Sodergren, S.; Siegbahn, H.; Rensmo, H.; Lindstrom, H.; Hagfeldt, A.; Lindquist, S. E. *J. Phys. Chem. B* **1997**, *101*, 3087−3090.
(38) Yu, J. G.; Yu, H. G.; Guo, H. T.; Li, M.; Mann, S. *Small* **2008**, *4*, 87−91.
(39) Chai, J. W.; Pan, J. S.; Wang, S. J.; Huan, C. H. A.; Lau, G. S.; Zheng, Y. B.; Xu, S. *Surf. Sci.* **2005**, *589*, 32−41.
(40) Zsoldos, Z.; Guczi, L. *J. Phys. Chem.* **1992**, *96*, 9393−9400.
(41) Kronik, L.; Shapira, Y. *Surf. Sci. Rep.* **1999**, *37*, 1−206.
(42) Lenzmann, F.; Krueger, J.; Burnside, S.; Brooks, K.; Grätzel, M.; Gal, D.; Ruhle, S.; Cahen, D. *J. Phys. Chem. B* **2001**, *105*, 6347−6452.
(43) Xin, B. F.; Jing, L. Q.; Ren, Z. Y.; Wang, B. Q.; Fu, H. G. *J. Phys. Chem. B* **2005**, *109*, 2805−2809.
(44) Wang, D. J.; Zhang, J.; Shi, T. S.; Wang, B. H.; Cao, X. Z.; Li, T. J. *J. Photochem. Photobiol. A* **1996**, *93*, 21−25.
(45) Pendlebury, S. R.; Barroso, M.; Cowan, A. J.; Sivula, K.; Tang, J.; Grätzel, M.; Klug, D. R.; Durrant, J. R. *Chem. Commun.* **2011**, *47*, 716−718.
(46) Daniel, A. L.; Yogesh, S.; Daniel, G. N. *J. Am. Chem. Soc.* **2009**, *131*, 3838−3839.
(47) Hensel, J.; Wang, G. M.; Li, Y.; Zhang, J. Z. *Nano Lett.* **2010**, *10*, 478−483.
(48) Steinmiller, E. M. P.; Kyoung-Shin, C. *Proc. Natl. Acad. Sci. U.S.A.* **2009**, *106*, 20633−20636.
(49) Yang, J.; Liu, H. W.; Martens, W. N.; Fros, R. L. *J. Phys. Chem. C* **2010**, *114*, 111−119.
(50) Barroso, M.; Cowan, A. J.; Pendlebury, S. R.; Grätzel, M.; Klug, D. R.; Durrant, J. R. *J. Am. Chem. Soc.* **2011**, *133*, 14868−14871.
(51) Tang, Q.; Zhou, W. J.; Shen, J. M.; Zhang, W.; Kong, L. F.; Qian, Y. T. *Chem. Commun.* **2004**, *6*, 712−713.
(52) Kundu, P.; Deshpande, P. A.; Madras, G.; Ravishankar, N. *J. Mater. Chem.* **2011**, *21*, 4209−4216.
(53) Hahn, N. T.; Mullins, C. B. *Chem. Mater.* **2010**, *22*, 6474−6482.
(54) Yu, J. G.; Yu, X. X.; Huang, B. B.; Zhang, X. Y.; Dai, Y. *Cryst. Growth Des.* **2009**, *9*, 1474−1480.
(55) Wang, D.; Li, R.; Zhu, J.; Shi, J. Y.; Han, J. F; Zong, X.; Li, C. *J. Phys. Chem. C* **2012**, *116*, 5082−5089.
(56) Wang, Y. B.; Wang, Y. S.; Jiang, R. R.; Xu, R. *Ind. Eng. Chem. Res.* **2012**, *51*, 9945−9951.